

Search for Cabibbo-suppressed decays $\Lambda_c^+ \rightarrow \Sigma^0 K^+ \pi^0$ and $\Lambda_c^+ \rightarrow \Sigma^0 K^+ \pi^+ \pi^-$

- M. Ablikim (麦迪娜)¹ M. N. Achasov^{4,c} P. Adlarson⁷⁶ X. C. Ai (艾小聪)⁸¹ R. Aliberti³⁵ A. Amoroso^{75A,75C}
 Q. An (安琪)^{72,58,a} Y. Bai (白羽)⁵⁷ O. Bakina³⁶ Y. Ban (班勇)^{46,h} H.-R. Bao (包浩然)⁶⁴ V. Batozskaya^{1,44}
 K. Begzsuren³² N. Berger³⁵ M. Berlowski⁴⁴ M. Bertani^{28A} D. Bettoni^{29A} F. Bianchi^{75A,75C} E. Bianco^{75A,75C}
 A. Bortone^{75A,75C} I. Boyko³⁶ R. A. Briere⁵ A. Brueggemann⁶⁹ H. Cai (蔡浩)⁷⁷ M. H. Cai (蔡铭航)^{38,k,l}
 X. Cai (蔡啸)^{1,58} A. Calcaterra^{28A} G. F. Cao (曹国富)^{1,64} N. Cao (曹宁)^{1,64} S. A. Cetin^{62A} X. Y. Chai (柴新宇)^{46,h}
 J. F. Chang (常劲帆)^{1,58} G. R. Che (车国荣)⁴³ Y. Z. Che (车逾之)^{1,58,64} G. Chelkov^{36,b} C. Chen (陈琛)⁴³
 C. H. Chen (陈春卉)⁹ Chao Chen (陈超)⁵⁵ G. Chen (陈刚)¹ H. S. Chen (陈和生)^{1,64} H. Y. Chen (陈弘扬)²⁰
 M. L. Chen (陈玛丽)^{1,58,64} S. J. Chen (陈申见)⁴² S. L. Chen (陈思璐)⁴⁵ S. M. Chen (陈少敏)⁶¹ T. Chen (陈通)^{1,64}
 X. R. Chen (陈旭荣)^{31,64} X. T. Chen (陈肖婷)^{1,64} Y. B. Chen (陈元柏)^{1,58} Y. Q. Chen³⁴ Z. J. Chen (陈卓俊)^{25,i}
 Z. K. Chen (陈梓康)⁵⁹ S. K. Choi¹⁰ X. Chu (初晓)^{12,g} G. Cibinetto^{29A} F. Cossio^{75C} J. J. Cui (崔佳佳)⁵⁰
 H. L. Dai (代洪亮)^{1,58} J. P. Dai (代建平)⁷⁹ A. Dbeysi¹⁸ R. E. de Boer³ D. Dedovich³⁶ C. Q. Deng (邓创旗)⁷³
 Z. Y. Deng (邓子艳)¹ A. Denig³⁵ I. Denysenko³⁶ M. Destefanis^{75A,75C} F. De Mori^{75A,75C} B. Ding (丁彪)^{67,1}
 X. X. Ding (丁晓萱)^{46,h} Y. Ding (丁逸)³⁴ Y. Ding (丁勇)⁴⁰ Y. X. Ding (丁玉鑫)³⁰ J. Dong (董静)^{1,58}
 L. Y. Dong (董燎原)^{1,64} M. Y. Dong (董明义)^{1,58,64} X. Dong (董翔)⁷⁷ M. C. Du (杜蒙川)¹ S. X. Du (杜书先)⁸¹
 Y. Y. Duan (段尧予)⁵⁵ Z. H. Duan (段宗欢)⁴² P. Egorov^{36,b} G. F. Fan (樊高峰)⁴² J. J. Fan (樊俊杰)¹⁹
 Y. H. Fan (范宇晗)⁴⁵ J. Fang (方进)⁵⁹ J. Fang (方建)^{1,58} S. S. Fang (房双世)^{1,64} W. X. Fang (方文兴)¹
 Y. Q. Fang (方亚泉)^{1,58} R. Farinelli^{29A} L. Fava^{75B,75C} F. Feldbauer³ G. Felici^{28A} C. Q. Feng (封常青)^{72,58}
 J. H. Feng (冯俊华)⁵⁹ Y. T. Feng (冯筠潼)^{72,58} M. Fritsch³ C. D. Fu (傅成栋)¹ J. L. Fu (傅金林)⁶⁴
 Y. W. Fu (傅亦威)^{1,64} H. Gao (高涵)⁶⁴ X. B. Gao (高鑫博)⁴¹ Y. N. Gao (高语浓)¹⁹ Y. N. Gao (高原宁)^{46,h}
 Y. Y. Gao (高洋洋)³⁰ Yang Gao (高扬)^{72,58} S. Garbolino^{75C} I. Garzia^{29A,29B} P. T. Ge (葛潘婷)¹⁹ Z. W. Ge (葛振武)⁴²
 C. Geng (耿聪)⁵⁹ E. M. Gersabeck⁶⁸ A. Gilman⁷⁰ K. Goetzen¹³ L. Gong (龚丽)⁴⁰ W. X. Gong (龚文煊)^{1,58}
 W. Gradl³⁵ S. Gramigna^{29A,29B} M. Greco^{75A,75C} M. H. Gu (顾旻皓)^{1,58} Y. T. Gu (顾运厅)¹⁵ C. Y. Guan (关春懿)^{1,64}
 A. Q. Guo (郭爱强)³¹ L. B. Guo (郭立波)⁴¹ M. J. Guo (国梦娇)⁵⁰ R. P. Guo (郭如盼)⁴⁹ Y. P. Guo (郭玉萍)^{12,g}
 A. Guskov^{36,b} J. Gutierrez²⁷ K. L. Han (韩坤霖)⁶⁴ T. T. Han (韩婷婷)¹ F. Hanisch³ K. D. Hao (郝科迪)^{72,58}
 X. Q. Hao (郝喜庆)¹⁹ F. A. Harris⁶⁶ K. K. He (何凯凯)⁵⁵ K. L. He (何康林)^{1,64} F. H. Heinsius³ C. H. Heinz³⁵
 Y. K. Heng (衡月昆)^{1,58,64} C. Herold⁶⁰ T. Holtmann³ P. C. Hong (洪鹏程)³⁴ G. Y. Hou (侯国一)^{1,64}
 X. T. Hou (侯贤涛)^{1,64} Y. R. Hou (侯颖锐)⁶⁴ Z. L. Hou (侯治龙)¹ B. Y. Hu (胡碧颖)⁵⁹ H. M. Hu (胡海明)^{1,64}
 J. F. Hu (胡继峰)^{56,j} Q. P. Hu (胡启鹏)^{72,58} S. L. Hu (胡圣亮)^{12,g} T. Hu (胡涛)^{1,58,64} Y. Hu (胡誉)¹
 Z. M. Hu (胡忠敏)⁵⁹ G. S. Huang (黄光顺)^{72,58} K. X. Huang (黄凯旋)⁵⁹ L. Q. Huang (黄麟钦)^{31,64} P. Huang (黄盼)⁴²
 X. T. Huang (黄性涛)⁵⁰ Y. P. Huang (黄燕萍)¹ Y. S. Huang (黄永盛)⁵⁹ T. Hussain⁷⁴ N. Hüsken³⁵

Received 16 February 2025; Accepted 2 April 2025; Published online 3 April 2025

* This study has been supported in part by National Key R&D Program of China (2020YFA0406300, 2020YFA0406400, 2023YFA1606000); National Natural Science Foundation of China (NSFC) (12205141, 11635010, 11735014, 11935015, 11935016, 11935018, 12025502, 12035009, 12035013, 12061131003, 12192260, 12192261, 12192262, 12192263, 12192264, 12192265, 12221005, 12225509, 12235017, 12361141819); Natural Science Foundation of Hunan Province (2024JJ2044); the Chinese Academy of Sciences (CAS) Large-Scale Scientific Facility Program; the CAS Center for Excellence in Particle Physics (CCEPP); Joint Large-Scale Scientific Facility Funds of the NSFC and CAS (U1832207); 100 Talents Program of CAS; The Institute of Nuclear and Particle Physics (INPAC) and Shanghai Key Laboratory for Particle Physics and Cosmology; German Research Foundation DFG (FOR5327); Istituto Nazionale di Fisica Nucleare, Italy; Knut and Alice Wallenberg Foundation (2021.0174, 2021.0299); Ministry of Development of Turkey (DPT2006K-120470); National Research Foundation of Korea (NRF-2022R1A2C1092335); National Science and Technology fund of Mongolia; National Science Research and Innovation Fund (NSRF) via the Program Management Unit for Human Resources & Institutional Development, Research and Innovation of Thailand (B16F640076, B50G670107); Polish National Science Centre (2019/35/O/ST2/02907); Swedish Research Council (2019.04595); The Swedish Foundation for International Cooperation in Research and Higher Education (CH2018-7756); and U. S. Department of Energy (DE-FG02-05ER41374).

 Content from this work may be used under the terms of the Creative Commons Attribution 3.0 licence. Any further distribution of this work must maintain attribution to the author(s) and the title of the work, journal citation and DOI. Article funded by SCOAP³ and published under licence by Chinese Physical Society and the Institute of High Energy Physics of the Chinese Academy of Sciences and the Institute of Modern Physics of the Chinese Academy of Sciences and IOP Publishing Ltd

- N. in der Wiesche⁶⁹ J. Jackson²⁷ S. Janchiv³² Q. Ji (纪全)¹ Q. P. Ji (姬清平)¹⁹ W. Ji (季旺)^{1,64} X. B. Ji (季晓斌)^{1,64}
 X. L. Ji (季筱璐)^{1,58} Y. Y. Ji (吉钰瑶)⁵⁰ Z. K. Jia (贾泽坤)^{72,58} D. Jiang (姜地)^{1,64} H. B. Jiang (姜候兵)⁷⁷
 P. C. Jiang (蒋沛成)^{46,h} S. J. Jiang (蒋思婧)⁹ T. J. Jiang (蒋庭俊)¹⁶ X. S. Jiang (江晓山)^{1,58,64} Y. Jiang (蒋艺)⁶⁴
 J. B. Jiao (焦健斌)⁵⁰ J. K. Jiao (焦俊坤)³⁴ Z. Jiao (焦铮)²³ S. Jin (金山)⁴² Y. Jin (金毅)⁶⁷ M. Q. Jing (荆茂强)^{1,64}
 X. M. Jing (景新媚)⁶⁴ T. Johansson⁷⁶ S. Kabana³³ N. Kalantar-Nayestanaki⁶⁵ X. L. Kang (康晓琳)⁹
 X. S. Kang (康晓珅)⁴⁰ M. Kavatsyuk⁶⁵ B. C. Ke (柯百谦)⁸¹ V. Khachatryan²⁷ A. Khoukaz⁶⁹ R. Kiuchi¹
 O. B. Kolcu^{62A} B. Kopf⁸ M. Kuessner³ X. Kui (奎贤)^{1,64} N. Kumar²⁶ A. Kupsc^{44,76} W. Kühn³⁷ Q. Lan (兰强)⁷³
 W. N. Lan (兰文宁)¹⁹ T. T. Lei (雷天天)^{72,58} Z. H. Lei (雷祚弘)^{72,58} M. Lellmann³⁵ T. Lenz³⁵ C. Li (李翠)⁴⁷
 C. Li (李聪)⁴³ C. H. Li (李春花)³⁹ C. K. Li (李春凯)²⁰ Cheng Li (李澄)^{72,58} D. M. Li (李德民)⁸¹ F. Li (李飞)^{1,58}
 G. Li (李刚)¹ H. B. Li (李海波)^{1,64} H. J. Li (李惠静)¹⁹ H. N. Li (李衡讷)^{56,j} Hui Li (李慧)⁴³ J. R. Li (李嘉荣)⁶¹
 J. S. Li (李静舒)⁵⁹ K. Li (李科)¹ K. L. Li (李凯璐)¹⁹ K. L. Li (李凯璐)^{38,k,l} L. J. Li (李林健)^{1,64} Lei Li (李蕾)⁴⁸
 M. H. Li (李明浩)⁴³ M. R. Li (李明润)^{1,64} P. L. Li (李佩莲)⁶⁴ P. R. Li (李培荣)^{38,k,l} Q. M. Li (李启铭)^{1,64}
 Q. X. Li (李起鑫)⁵⁰ R. Li (李燃)^{17,31} T. Li (李腾)⁵⁰ T. Y. Li (李天佑)⁴³ W. D. Li (李卫东)^{1,64} W. G. Li (李卫国)^{1,a}
 X. Li (李旭)^{1,64} X. H. Li (李旭红)^{72,58} X. L. Li (李晓玲)⁵⁰ X. Y. Li (李晓宇)^{1,8} X. Z. Li (李绪泽)⁵⁹ Y. Li (李洋)¹⁹
 Y. G. Li (李彦谷)^{46,h} Z. J. Li (李志军)⁵⁹ Z. Y. Li (李紫阳)⁷⁹ C. Liang (梁畅)⁴² H. Liang (梁昊)^{72,58}
 Y. F. Liang (梁勇飞)⁵⁴ Y. T. Liang (梁羽铁)^{31,64} G. R. Liao (廖广睿)¹⁴ L. B. Liao (廖立波)⁵⁹ M. H. Liao (廖明华)⁵⁹
 Y. P. Liao (廖一朴)^{1,64} J. Libby²⁶ A. Limphirat⁶⁰ C. C. Lin (蔺长城)⁵⁵ C. X. Lin (林创新)⁶⁴ D. X. Lin (林德旭)^{31,64}
 L. Q. Lin (邵麟筌)³⁹ T. Lin (林韬)¹ B. J. Liu (刘北江)¹ B. X. Liu (刘宝鑫)⁷⁷ C. Liu (刘成)³⁴ C. X. Liu (刘春秀)¹
 F. Liu (刘芳)¹ F. H. Liu (刘福虎)⁵³ Feng Liu (刘峰)⁶ G. M. Liu (刘国明)^{56,j} H. Liu (刘昊)^{38,k,l}
 H. B. Liu (刘宏邦)¹⁵ H. H. Liu (刘欢欢)¹ H. M. Liu (刘怀民)^{1,64} Huihui Liu (刘汇慧)²¹ J. B. Liu (刘建北)^{72,58}
 J. J. Liu (刘佳佳)²⁰ K. Liu (刘凯)^{38,k,l} K. Liu (刘坤)⁷³ K. Y. Liu (刘魁勇)⁴⁰ Ke Liu (刘珂)²² L. Liu (刘亮)^{72,58}
 L. C. Liu (刘良辰)⁴³ Lu Liu (刘露)⁴³ M. H. Liu (刘美宏)^{12,g} P. L. Liu (刘佩莲)¹ Q. Liu (刘倩)⁶⁴
 S. B. Liu (刘树彬)^{72,58} T. Liu (刘桐)^{12,g} W. K. Liu (刘维克)⁴³ W. M. Liu (刘卫民)^{72,58} W. T. Liu (刘婉婷)³⁹
 X. Liu (刘鑫)³⁹ X. Liu (刘翔)^{38,k,l} X. Y. Liu (刘雪吟)⁷⁷ Y. Liu (刘媛)⁸¹ Y. Liu (刘义)⁸¹ Y. Liu (刘英)^{38,k,l}
 Y. B. Liu (刘玉斌)⁴³ Z. A. Liu (刘振安)^{1,58,64} Z. D. Liu (刘宗德)⁹ Z. Q. Liu (刘智青)⁵⁰ X. C. Lou (娄辛丑)^{1,58,64}
 F. X. Lu (卢飞翔)⁵⁹ H. J. Lu (吕海江)²³ J. G. Lu (吕军光)^{1,58} Y. Lu (卢宇)⁷ Y. H. Lu (卢泱宏)^{1,64}
 Y. P. Lu (卢云鹏)^{1,58} Z. H. Lu (卢泽辉)^{1,64} C. L. Luo (罗成林)⁴¹ J. R. Luo (罗家瑞)⁵⁹ J. S. Luo (罗家顺)^{1,64}
 M. X. Luo (罗民兴)⁸⁰ T. Luo (罗涛)^{12,g} X. L. Luo (罗小兰)^{1,58} X. R. Lyu (吕晓睿)^{64,p} Y. F. Lyu (吕翌丰)⁴³
 Y. H. Lyu (吕云鹤)⁸¹ F. C. Ma (马凤才)⁴⁰ H. Ma (马衡)⁷⁹ H. L. Ma (马海龙)¹ J. L. Ma (马俊力)^{1,64}
 L. L. Ma (马连良)⁵⁰ L. R. Ma (马立瑞)⁶⁷ Q. M. Ma (马秋梅)¹ R. Q. Ma (马润秋)^{1,64} R. Y. Ma (马若云)¹⁹
 T. Ma (马腾)^{72,58} X. T. Ma (马晓天)^{1,64} X. Y. Ma (马骁妍)^{1,58} Y. M. Ma (马玉明)³¹ F. E. Maas¹⁸ I. MacKay⁷⁰
 M. Maggiora^{75A,75C} S. Malde⁷⁰ Y. J. Mao (冒亚军)^{46,h} Z. P. Mao (毛泽普)¹ S. Marcello^{75A,75C}
 Y. H. Meng (孟琰皓)⁶⁴ Z. X. Meng (孟召霞)⁶⁷ J. G. Messchendorp^{13,65} G. Mezzadri^{29A} H. Miao (妙晗)^{1,64}
 T. J. Min (闵天觉)⁴² R. E. Mitchell²⁷ X. H. Mo (莫晓虎)^{1,58,64} B. Moses²⁷ N. Yu. Muchnoi^{4,c} J. Muskalla³⁵
 Y. Nefedov³⁶ F. Nerling^{18,e} L. S. Nie (聂麟苏)²⁰ I. B. Nikolaev^{4,c} Z. Ning (宁哲)^{1,58} S. Nisar^{11,m}
 Q. L. Niu (牛祺乐)^{38,k,l} S. L. Olsen^{10,64} Q. Ouyang (欧阳群)^{1,58,64} S. Pacetti^{28B,28C} X. Pan (潘祥)⁵⁵ Y. Pan (潘越)⁵⁷
 A. Pathak¹⁰ Y. P. Pei (裴宇鹏)^{72,58} M. Pelizaeus³ H. P. Peng (彭海平)^{72,58} Y. Y. Peng (彭云翊)^{38,k,l} K. Peters^{13,e}
 J. L. Ping (平加伦)⁴¹ R. G. Ping (平荣刚)^{1,64} S. Plura³⁵ V. Prasad³³ F. Z. Qi (齐法制)¹ H. R. Qi (漆红荣)⁶¹
 M. Qi (祁鸣)⁴² S. Qian (钱森)^{1,58} W. B. Qian (钱文斌)⁶⁴ C. F. Qiao (乔从丰)⁶⁴ J. H. Qiao (乔佳辉)¹⁹
 J. J. Qin (秦佳佳)^{73,1D} J. L. Qin (覃嘉良)⁵⁵ L. Q. Qin (秦丽清)¹⁴ L. Y. Qin (秦龙宇)^{72,58} P. B. Qin (秦鹏勃)⁷³
 X. P. Qin (覃潇平)^{12,g} X. S. Qin (秦小帅)⁵⁰ Z. H. Qin (秦中华)^{1,58} J. F. Qiu (邱进发)¹ Z. H. Qu (屈子皓)⁷³
 C. F. Redmer³⁵ A. Rivetti^{75C} M. Rolo^{75C} G. Rong (荣刚)^{1,64} S. S. Rong (荣少石)^{1,64} Ch. Rosner¹⁸
 M. Q. Ruan (阮曼奇)^{1,58} S. N. Ruan (阮氏宁)⁴³ N. Salone⁴⁴ A. Sarantsev^{36,d} Y. Schelhaas³⁵ K. Schoenning⁷⁶
 M. Scogeggio^{29A} K. Y. Shan (尚科羽)^{12,g} W. Shan (单蔚)²⁴ X. Y. Shan (单心钰)^{72,58} Z. J. Shang (尚子杰)^{38,k,l}
 J. F. Shangguan (上官剑锋)¹⁶ L. G. Shao (邵立港)^{1,64} M. Shao (邵明)^{72,58} C. P. Shen (沈成平)^{12,g}
 H. F. Shen (沈宏飞)^{1,8} W. H. Shen (沈文涵)⁶⁴ X. Y. Shen (沈肖雁)^{1,64} B. A. Shi (施伯安)⁶⁴ H. Shi (史华)^{72,58}

- J. L. Shi (石家磊)^{12,g} J. Y. Shi (石京燕)¹ S. Y. Shi (史书宇)⁷³ X. Shi (史欣)^{1,58} H. L. Song (宋海林)^{72,58}
 J. J. Song (宋娇娇)¹⁹ T. Z. Song (宋天资)⁵⁹ W. M. Song (宋维民)^{34,1} Y. J. Song (宋宇镜)^{12,g}
 Y. X. Song (宋昀轩)^{46,h,n} S. Sosio^{75A,75C} S. Spataro^{75A,75C} F. Stieler³⁵ S. S Su (苏闪闪)⁴⁰ Y. J. Su (粟杨捷)⁶⁴
 G. B. Sun (孙光豹)⁷⁷ G. X. Sun (孙功星)¹ H. Sun (孙昊)⁶⁴ H. K. Sun (孙浩凯)¹ J. F. Sun (孙俊峰)¹⁹
 K. Sun (孙开)⁶¹ L. Sun (孙亮)⁷⁷ S. S. Sun (孙胜森)^{1,64} T. Sun^{51,f} Y. C. Sun (孙雨长)⁷⁷ Y. H. Sun (孙益华)³⁰
 Y. J. Sun (孙勇杰)^{72,58} Y. Z. Sun (孙永昭)¹ Z. Q. Sun (孙泽群)^{1,64} Z. T. Sun (孙振田)⁵⁰ C. J. Tang (唐昌建)⁵⁴
 G. Y. Tang (唐光毅)¹ J. Tang (唐健)⁵⁹ L. F. Tang (唐林发)³⁹ M. Tang (唐嘉骏)^{72,58} Y. A. Tang (唐迎澳)⁷⁷
 L. Y. Tao (陶璐燕)⁷³ M. Tat⁷⁰ J. X. Teng (滕佳秀)^{72,58} V. Thoren⁷⁶ J. Y. Tian (田济源)^{72,58} W. H. Tian (田文辉)⁵⁹
 Y. Tian (田野)³¹ Z. F. Tian (田喆飞)⁷⁷ I. Uman^{62B} B. Wang (王斌)¹ B. Wang (王博)⁵⁹ Bo Wang (王博)^{72,58}
 C. Wang (王超)¹⁹ D. Y. Wang (王大勇)^{46,h} H. J. Wang (王泓鉴)^{38,k,l} J. J. Wang (王家驹)⁷⁷ K. Wang (王科)^{1,58}
 L. L. Wang (王亮亮)¹ L. W. Wang (王璐仪)³⁴ M. Wang (王萌)⁵⁰ M. Wang^{72,58} N. Y. Wang (王南洋)⁶⁴
 S. Wang (王石)^{38,k,l} S. Wang (王顺)^{12,g} T. Wang (王婷)^{12,g} T. J. Wang (王腾蛟)⁴³ W. Wang (王维)⁷³
 W. Wang (王为)⁵⁹ W. P. Wang (王维平)^{35,58,72,o} X. Wang (王轩)^{46,h} X. F. Wang (王雄飞)^{38,k,l} X. J. Wang (王希俊)³⁹
 X. L. Wang (王小龙)^{12,g} X. N. Wang (王新南)¹ Y. Wang (王亦)⁶¹ Y. D. Wang (王雅迪)⁴⁵ Y. F. Wang (王贻芳)^{1,58,64}
 Y. H. Wang (王英豪)^{38,k,l} Y. L. Wang (王艺龙)¹⁹ Y. N. Wang (王燕宁)⁷⁷ Y. Q. Wang (王雨晴)¹
 Yaqian Wang (王亚乾)¹⁷ Yi Wang (王义)⁶¹ Yuan Wang (王源)^{17,31} Z. Wang (王铮)^{1,58} Z. L. Wang (王治浪)⁷³
 Z. Y. Wang (王至勇)^{1,64} D. H. Wei (魏代会)¹⁴ F. Weidner⁶⁹ S. P. Wen (文硕频)¹ Y. R. Wen (温亚冉)³⁹
 U. Wiedner³ G. Wilkinson⁷⁰ M. Wolke⁷⁶ C. Wu (吴晨)³⁹ J. F. Wu (吴金飞)^{1,8} L. H. Wu (伍灵慧)¹
 L. J. Wu (吴连近)^{1,64} Lianjie Wu (武廉杰)¹⁹ S. G. Wu (吴韶光)^{1,64} S. M. Wu (吴蜀明)⁶⁴ X. Wu (吴潇)^{12,g}
 X. H. Wu (伍雄浩)³⁴ Y. J. Wu (吴英杰)³¹ Z. Wu (吴智)^{1,58} L. Xia (夏磊)^{72,58} X. M. Xian (咸秀梅)³⁹
 B. H. Xiang (向本后)^{1,64} T. Xiang (相腾)^{46,h} D. Xiao (肖栋)^{38,k,l} G. Y. Xiao (肖光延)⁴² H. Xiao (肖浩)⁷³
 Y. L. Xiao (肖云龙)^{12,g} Z. J. Xiao (肖振军)⁴¹ C. Xie (谢陈)⁴² K. J. Xie (谢凯吉)^{1,64} X. H. Xie (谢昕海)^{46,h}
 Y. Xie (谢勇)⁵⁰ Y. G. Xie (谢宇广)^{1,58} Y. H. Xie (谢跃红)⁶ Z. P. Xie (谢智鹏)^{72,58} T. Y. Xing (邢天宇)^{1,64}
 C. F. Xu^{1,64} C. J. Xu (许创杰)⁵⁹ G. F. Xu (许国发)¹ M. Xu (徐明)^{72,58} Q. J. Xu (徐庆君)¹⁶ Q. N. Xu³⁰
 W. L. Xu (徐万伦)⁶⁷ X. P. Xu (徐新平)⁵⁵ Y. Xu (徐月)⁴⁰ Y. C. Xu (胥英超)⁷⁸ Z. S. Xu (许昭燊)⁶⁴
 F. Yan (严芳)^{12,g} H. Y. Yan (闫浩宇)³⁹ L. Yan (严亮)^{12,g} W. B. Yan (鄢文标)^{72,58} W. C. Yan (闫文成)⁸¹
 W. P. Yan (闫文鹏)¹⁹ X. Q. Yan (严薛强)^{1,64} H. J. Yang (杨海军)^{51,f} H. L. Yang (杨昊霖)³⁴ H. X. Yang (杨洪勋)¹
 J. H. Yang (杨君辉)⁴² R. J. Yang (杨润佳)¹⁹ T. Yang (杨涛)¹ Y. Yang (杨莹)^{12,g} Y. F. Yang (杨艳芳)⁴³
 Y. Q. Yang (杨永强)⁹ Y. X. Yang (杨逸翔)^{1,64} Y. Z. Yang (杨颖皓)¹⁹ M. Ye (叶梅)^{1,58} M. H. Ye (叶铭汉)⁸
 Junhao Yin (殷俊昊)⁴³ Z. Y. You (尤郑昀)⁵⁹ B. X. Yu (俞伯祥)^{1,58,64} C. X. Yu (喻纯旭)⁴³ G. Yu¹³
 J. S. Yu (俞洁晟)^{25,i} M. C. Yu⁴⁰ T. Yu (于涛)⁷³ X. D. Yu (余旭东)^{46,h} Y. C. Yu (郁烨淳)⁸¹ C. Z. Yuan (苑长征)^{1,64}
 H. Yuan (袁昊)^{1,64} J. Yuan (袁菁)³⁴ J. Yuan (袁杰)⁴⁵ L. Yuan (袁丽)² S. C. Yuan (苑思成)^{1,64} Y. Yuan (袁野)^{1,64}
 Z. Y. Yuan (袁朝阳)⁵⁹ C. X. Yue (岳崇兴)³⁹ Ying Yue (岳颖)¹⁹ A. A. Zafar⁷⁴ S. H. Zeng^{63A,63B,63C,63D}
 X. Zeng (曾鑫)^{12,g} Y. Zeng (曾云)^{25,i} Y. J. Zeng (曾宇杰)⁵⁹ Y. J. Zeng (曾溢嘉)^{1,64} X. Y. Zhai (翟星晔)³⁴
 Y. H. Zhan (詹永华)⁵⁹ A. Q. Zhang (张安庆)^{1,64} B. L. Zhang (张伯伦)^{1,64} B. X. Zhang (张丙新)¹
 D. H. Zhang (张丹昊)⁴³ G. Y. Zhang (张广义)¹⁹ G. Y. Zhang (张耕源)^{1,64} H. Zhang (张豪)^{72,58} H. Zhang (张晗)⁸¹
 H. C. Zhang (张航畅)^{1,58,64} H. H. Zhang (张宏浩)⁵⁹ H. Q. Zhang (张华桥)^{1,58,64} H. R. Zhang (张浩然)^{72,58}
 H. Y. Zhang (章红宇)^{1,58} J. Zhang (张晋)⁵⁹ J. Zhang (张进)⁸¹ J. J. Zhang (张进军)⁵² J. L. Zhang (张杰磊)²⁰
 J. Q. Zhang (张敬庆)⁴¹ J. S. Zhang (张家声)^{12,g} J. W. Zhang (张家文)^{1,58,64} J. X. Zhang (张景旭)^{38,k,l}
 J. Y. Zhang (张建勇)¹ J. Z. Zhang (张景芝)^{1,64} Jianyu Zhang (张剑宇)⁶⁴ L. M. Zhang (张黎明)⁶¹ Lei Zhang (张雷)⁴²
 N. Zhang (张楠)⁸¹ P. Zhang (张鹏)^{1,64} Q. Zhang (张强)¹⁹ Q. Y. Zhang (张秋岩)³⁴ R. Y. Zhang (张若愚)^{38,k,l}
 S. H. Zhang (张水涵)^{1,64} Shulei Zhang (张书磊)^{25,i} X. M. Zhang (张晓梅)¹ X. Y. Zhang⁴⁰ X. Y. Zhang (张学尧)⁵⁰
 Y. Zhang (张璠)¹ Y. Zhang (张宇)⁷³ Y. T. Zhang (张亚腾)⁸¹ Y. H. Zhang (张银鸿)^{1,58} Y. M. Zhang (张悦明)³⁹
 Z. D. Zhang (张正德)¹ Z. H. Zhang (张泽恒)¹ Z. L. Zhang (张志龙)⁵⁵ Z. L. Zhang (张兆领)³⁴
 Z. X. Zhang (张泽祥)¹⁹ Z. Y. Zhang (张振宇)⁷⁷ Z. Y. Zhang (张子羽)⁴³ Z. Z. Zhang (张子扬)⁴⁵ Zh. Zh. Zhang¹⁹
 G. Zhao (赵光)¹ J. Y. Zhao (赵静宜)^{1,64} J. Z. Zhao (赵京周)^{1,58} L. Zhao (赵玲)¹ Lei Zhao (赵雷)^{72,58}

M. G. Zhao (赵明刚)⁴³ N. Zhao (赵宁)⁷⁹ R. P. Zhao (赵若平)⁶⁴ S. J. Zhao (赵书俊)⁸¹ Y. B. Zhao (赵豫斌)^{1,58}
Y. L. Zhao (赵艳琳)⁵⁵ Y. X. Zhao (赵宇翔)^{31,64} Z. G. Zhao (赵政国)^{72,58} A. Zhemchugov^{36,b} B. Zheng (郑波)⁷³
B. M. Zheng (郑变敏)³⁴ J. P. Zheng (郑建平)^{1,58} W. J. Zheng (郑文静)^{1,64} X. R. Zheng (郑心如)¹⁹
Y. H. Zheng (郑阳恒)^{64,p} B. Zhong (钟彬)⁴¹ X. Zhong (钟鑫)⁵⁹ H. Zhou (周航)^{35,50,o} J. Y. Zhou (周佳莹)³⁴
S. Zhou (周帅)⁶ X. Zhou (周详)⁷⁷ X. K. Zhou (周晓康)⁶ X. R. Zhou (周小蓉)^{72,58} X. Y. Zhou (周兴玉)³⁹
Y. Z. Zhou (周袆卓)^{12,g} Z. C. Zhou (周章丞)²⁰ A. N. Zhu (朱傲男)⁶⁴ J. Zhu (朱江)⁴³ K. Zhu (朱凯)¹
K. J. Zhu (朱科军)^{1,58,64} K. S. Zhu (朱康帅)^{12,g} L. Zhu (朱林)³⁴ L. X. Zhu (朱琳萱)⁶⁴ S. H. Zhu (朱世海)⁷¹
T. J. Zhu (朱腾蛟)^{12,g} W. D. Zhu (朱稳定)⁴¹ W. J. Zhu (朱文静)¹ W. Z. Zhu (朱文卓)¹⁹ Y. C. Zhu (朱莹春)^{72,58}
Z. A. Zhu (朱自安)^{1,64} X. Y. Zhuang (庄新宇)⁴³ J. H. Zou (邹佳恒)¹ J. Zu (祖健)^{72,58}

(BESIII Collaboration)

¹Institute of High Energy Physics, Beijing 100049, China²Beihang University, Beijing 100191, China³Bochum Ruhr-University, D-44780 Bochum, Germany⁴Budker Institute of Nuclear Physics SB RAS (BINP), Novosibirsk 630090, Russia⁵Carnegie Mellon University, Pittsburgh, Pennsylvania 15213, USA⁶Central China Normal University, Wuhan 430079, China⁷Central South University, Changsha 410083, China⁸China Center of Advanced Science and Technology, Beijing 100190, China⁹China University of Geosciences, Wuhan 430074, China¹⁰Chung-Ang University, Seoul, 06974, Republic of Korea¹¹COMSATS University Islamabad, Lahore Campus, Defence Road, Off Raiwind Road, 54000 Lahore, Pakistan¹²Fudan University, Shanghai 200433, China¹³GSI Helmholtzcentre for Heavy Ion Research GmbH, D-64291 Darmstadt, Germany¹⁴Guangxi Normal University, Guilin 541004, China¹⁵Guangxi University, Nanning 530004, China¹⁶Hangzhou Normal University, Hangzhou 310036, China¹⁷Hebei University, Baoding 071002, China¹⁸Helmholtz Institute Mainz, Staudinger Weg 18, D-55099 Mainz, Germany¹⁹Henan Normal University, Xinxiang 453007, China²⁰Henan University, Kaifeng 475004, China²¹Henan University of Science and Technology, Luoyang 471003, China²²Henan University of Technology, Zhengzhou 450001, China²³Huangshan College, Huangshan 245000, China²⁴Hunan Normal University, Changsha 410081, China²⁵Hunan University, Changsha 410082, China²⁶Indian Institute of Technology Madras, Chennai 600036, India²⁷Indiana University, Bloomington, Indiana 47405, USA^{28A}INFN Laboratori Nazionali di Frascati, INFN Laboratori Nazionali di Frascati, I-00044, Frascati, Italy^{28B}INFN Laboratori Nazionali di Frascati, INFN Sezione di Perugia, I-06100, Perugia, Italy^{28C}INFN Laboratori Nazionali di Frascati, University of Perugia, I-06100, Perugia, Italy^{29A}INFN Sezione di Ferrara, INFN Sezione di Ferrara, I-44122, Ferrara, Italy^{29B}INFN Sezione di Ferrara, University of Ferrara, I-44122, Ferrara, Italy³⁰Inner Mongolia University, Hohhot 010021, China³¹Institute of Modern Physics, Lanzhou 730000, China³²Institute of Physics and Technology, Peace Avenue 54B, Ulaanbaatar 13330, Mongolia³³Instituto de Alta Investigación, Universidad de Tarapacá, Casilla 7D, Arica 1000000, Chile³⁴Jilin University, Changchun 130012, China³⁵Johannes Gutenberg University of Mainz, Johann-Joachim-Becher-Weg 45, D-55099 Mainz, Germany³⁶Joint Institute for Nuclear Research, 141980 Dubna, Moscow region, Russia³⁷Justus-Liebig-Universitaet Giessen, II. Physikalisches Institut, Heinrich-Buff-Ring 16, D-35392 Giessen, Germany³⁸Lanzhou University, Lanzhou 730000, China³⁹Liaoning Normal University, Dalian 116029, China⁴⁰Liaoning University, Shenyang 110036, China⁴¹Nanjing Normal University, Nanjing 210023, China⁴²Nanjing University, Nanjing 210093, China⁴³Nankai University, Tianjin 300071, China⁴⁴National Centre for Nuclear Research, Warsaw 02-093, Poland⁴⁵North China Electric Power University, Beijing 102206, China⁴⁶Peking University, Beijing 100871, China⁴⁷Qufu Normal University, Qufu 273165, China⁴⁸Renmin University of China, Beijing 100872, China⁴⁹Shandong Normal University, Jinan 250014, China⁵⁰Shandong University, Jinan 250100, China

⁵¹Shanghai Jiao Tong University, Shanghai 200240, China⁵²Shanxi Normal University, Linfen 041004, China⁵³Shanxi University, Taiyuan 030006, China⁵⁴Sichuan University, Chengdu 610064, China⁵⁵Soochow University, Suzhou 215006, China⁵⁶South China Normal University, Guangzhou 510006, China⁵⁷Southeast University, Nanjing 211100, China⁵⁸State Key Laboratory of Particle Detection and Electronics, Beijing 100049, Hefei 230026, China⁵⁹Sun Yat-Sen University, Guangzhou 510275, China⁶⁰Suranaree University of Technology, University Avenue 111, Nakhon Ratchasima 30000, Thailand⁶¹Tsinghua University, Beijing 100084, China^{62A}Turkish Accelerator Center Particle Factory Group, Istinye University, 34010, Istanbul, Turkey^{62B}Turkish Accelerator Center Particle Factory Group, Near East University, Nicosia, North Cyprus, 99138, Mersin 10, Turkey⁶³University of Bristol, H H Wills Physics Laboratory, Tyndall Avenue, Bristol, BS8 1TL, UK⁶⁴University of Chinese Academy of Sciences, Beijing 100049, China⁶⁵University of Groningen, NL-9747 AA Groningen, The Netherlands⁶⁶University of Hawaii, Honolulu, Hawaii 96822, USA⁶⁷University of Jinan, Jinan 250022, China⁶⁸University of Manchester, Oxford Road, Manchester, M13 9PL, United Kingdom⁶⁹University of Muenster, Wilhelm-Klemm-Strasse 9, 48149 Muenster, Germany⁷⁰University of Oxford, Keble Road, Oxford OX1 3RH, United Kingdom⁷¹University of Science and Technology Liaoning, Anshan 114051, China⁷²University of Science and Technology of China, Hefei 230026, China⁷³University of South China, Hengyang 421001, China⁷⁴University of the Punjab, Lahore-54590, Pakistan^{75A}University of Turin and INFN, University of Turin, I-10125, Turin, Italy^{75B}University of Turin and INFN, University of Eastern Piedmont, I-15121, Alessandria, Italy^{75C}University of Turin and INFN, INFN, I-10125, Turin, Italy⁷⁶Uppsala University, Box 516, SE-75120 Uppsala, Sweden⁷⁷Wuhan University, Wuhan 430072, China⁷⁸Yantai University, Yantai 264005, China⁷⁹Yunnan University, Kunming 650500, China⁸⁰Zhejiang University, Hangzhou 310027, China⁸¹Zhengzhou University, Zhengzhou 450001, China^aDeceased^bAlso at the Moscow Institute of Physics and Technology, Moscow 141700, Russia^cAlso at the Novosibirsk State University, Novosibirsk, 630090, Russia^dAlso at the NRC "Kurchatov Institute", PNPI, 188300, Gatchina, Russia^eAlso at Goethe University Frankfurt, 60323 Frankfurt am Main, Germany^fAlso at Key Laboratory for Particle Physics, Astrophysics and Cosmology, Ministry of Education; Shanghai Key Laboratory for Particle Physics and Cosmology; Institute of Nuclear and Particle Physics, Shanghai 200240, China^gAlso at Key Laboratory of Nuclear Physics and Ion-beam Application (MOE) and Institute of Modern Physics, Fudan University, Shanghai 200443, China^hAlso at State Key Laboratory of Nuclear Physics and Technology, Peking University, Beijing 100871, ChinaⁱAlso at School of Physics and Electronics, Hunan University, Changsha 410082, China^jAlso at Guangdong Provincial Key Laboratory of Nuclear Science, Institute of Quantum Matter, South China Normal University, Guangzhou 510006, China^kAlso at MOE Frontiers Science Center for Rare Isotopes, Lanzhou University, Lanzhou 730000, China^lAlso at Lanzhou Center for Theoretical Physics, Lanzhou University, Lanzhou 730000, China^mAlso at the Department of Mathematical Sciences, IBA, Karachi 75270, PakistanⁿAlso at Ecole Polytechnique Federale de Lausanne (EPFL), CH-1015 Lausanne, Switzerland^oAlso at Helmholtz Institute Mainz, Staudinger Weg 18, D-55099 Mainz, Germany^pAlso at Hangzhou Institute for Advanced Study, University of Chinese Academy of Sciences, Hangzhou 310024, China

Abstract: Utilizing 4.5 fb^{-1} of e^+e^- annihilation data collected at center-of-mass energies ranging from 4599.53 MeV to 4698.82 MeV by the BESIII detector at the BEPCII collider, we searched for singly Cabibbo-suppressed hadronic decays $\Lambda_c^+ \rightarrow \Sigma^0 K^+ \pi^0$ and $\Lambda_c^+ \rightarrow \Sigma^0 K^+ \pi^+ \pi^-$ with a single-tag method. No significant signals were observed for both decays. The upper limits on the branching fractions at the 90% confidence level were determined to be 5.0×10^{-4} for $\Lambda_c^+ \rightarrow \Sigma^0 K^+ \pi^0$ and 6.5×10^{-4} for $\Lambda_c^+ \rightarrow \Sigma^0 K^+ \pi^+ \pi^-$.

Keywords: Charmed baryon, SCS decay, BESIII Experiment

DOI: 10.1088/1674-1137/adc88d **CSTR:** 32044.14.ChinesePhysicsC.49073001

I. INTRODUCTION

The experimental investigation of the decays of charmed baryons plays a critical role in understanding the complex dynamics of strong and weak interactions involving heavy quarks. The charmed baryon, Λ_c^+ , was first observed by the Mark II experiment in 1979 [1]. However, after decades of research, the sum of the known Λ_c^+ decay branching fractions (BFs) is still limited to approximately 70%, with the remaining decays yet to be measured [2, 3]. The hadronic decay amplitudes of Λ_c^+ include both factorizable and nonfactorizable contributions [4], given that its weak decays are not suppressed by color or helicity [5]. These nonfactorizable effects, such as those from W -exchange diagrams, play a crucial role in understanding the decay dynamics. In contrast, these effects are negligible in heavy meson decays [6]. Improving measurements of the BFs of Λ_c^+ decays is essential for better understanding the internal dynamics of charmed baryon decays.

Study of the three-body hadronic decays $\Lambda_c^+ \rightarrow B_n PP'$ is an important research area; B_n and $P(P')$ denote an octet baryon and a pseudoscalar meson, respectively. To date, Cabibbo-suppressed (SCS) hadronic decay $\Lambda_c^+ \rightarrow \Sigma^0 K^+ \pi^0$ has not been observed. This decay can proceed via the Feynman diagrams shown in Fig. 1. Predictions of the decay BF range from 0.8×10^{-3} to 1.2×10^{-3} with the $SU(3)$ flavor symmetry framework [7–9], under the assumption that the PP' system is in an S -wave state. The most recent prediction, reported in Ref. [9], considers the complete effective Hamiltonian contribution. By contrast, Ref. [10] predicts the BF of $\Lambda_c^+ \rightarrow \Sigma^0 K^+ \pi^0$ to be $(2.1 \pm 0.6) \times 10^{-3}$ using the statistical isospin model. Experimentally, the BESIII experiment searched for this decay for the first time using a double-tag method and set the upper limit on its BF at the 90% confidence level (C.L.) to be 1.8×10^{-3} [11].

Currently, there are no theoretical predictions of the four-body hadronic decay $\Lambda_c^+ \rightarrow \Sigma^0 K^+ \pi^+ \pi^-$. The BaBar experiment performed the first search for this decay and reported an upper limit on the BF ratio expressed as $\frac{\mathcal{B}(\Lambda_c^+ \rightarrow \Sigma^0 K^+ \pi^+ \pi^-)}{\mathcal{B}(\Lambda_c^+ \rightarrow \Sigma^0 \pi^+)} < 2.0 \times 10^{-2}$ at the 90% C.L. [12].

In this study, we searched for hadronic decays $\Lambda_c^+ \rightarrow \Sigma^0 K^+ \pi^0$ and $\Lambda_c^+ \rightarrow \Sigma^0 K^+ \pi^+ \pi^-$, with subsequent decays $\Sigma^0 \rightarrow \gamma \Lambda$ and $\Lambda \rightarrow p \pi^-$, utilizing 4.5 fb^{-1} of $e^+ e^-$ annihilation data collected at center-of-mass (c.m.) energies ranging from 4599.53 MeV to 4698.82 MeV [13–15]. The results could be employed to test theoretical models and provide important input to them. Throughout this paper, the charge-conjugate state is always implied.

II. BESIII DETECTOR AND MONTE CARLO SIMULATION

The BESIII detector [16] records symmetric $e^+ e^-$ col-

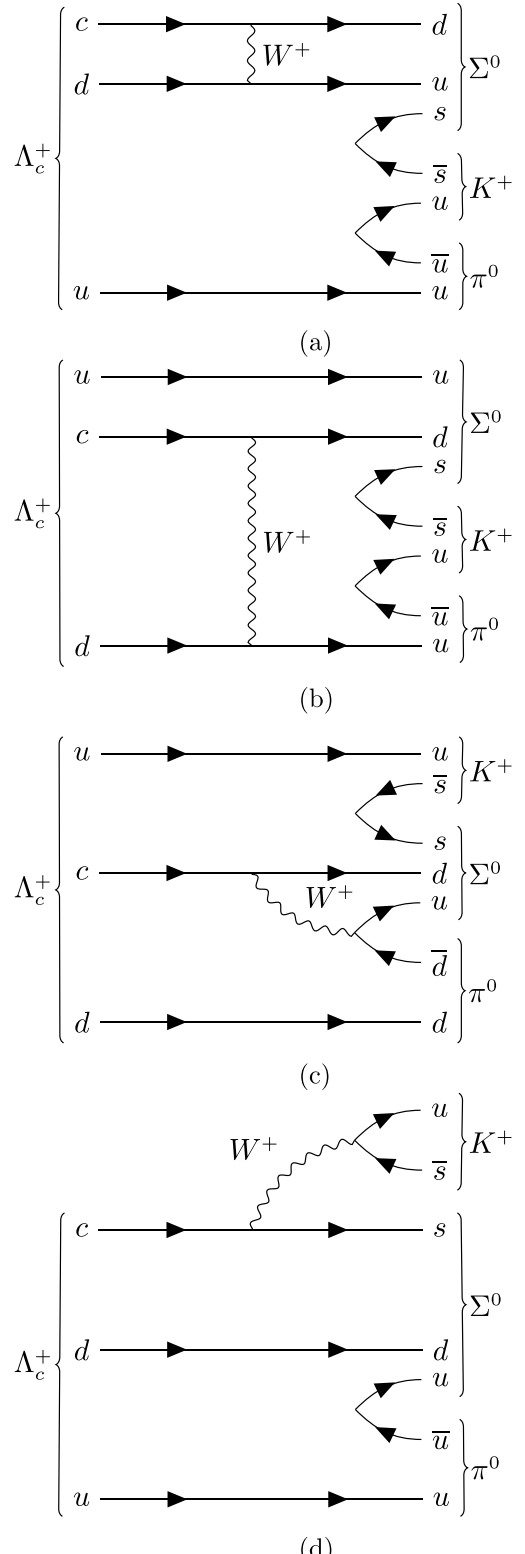


Fig. 1. Feynman diagrams of $\Lambda_c^+ \rightarrow \Sigma^0 K^+ \pi^0$: (a) and (b) W -exchange diagrams, (c) internal W -emission diagram, and (d) external W -emission diagram.

lisions provided by the BEPCII storage ring [17] in the c.m. energy range from 1.84 to 4.95 GeV, with a peak lu-

minosity of $1.1 \times 10^{33} \text{ cm}^{-2}\text{s}^{-1}$ achieved at $\sqrt{s} = 3.773 \text{ GeV}$. BESIII has collected large data samples in this energy region [21]. The cylindrical core of the BESIII detector covers 93% of the full solid angle and consists of a helium-based multilayer drift chamber (MDC), a plastic scintillator time-of-flight system (TOF), and a CsI(Tl) electromagnetic calorimeter (EMC), which are all enclosed in a superconducting solenoidal magnet providing a 1.0 T magnetic field. The solenoid is supported by an octagonal flux-return yoke with resistive plate counter muon identification modules interleaved with steel. The charged-particle momentum resolution at $1 \text{ GeV}/c$ is 0.5%, and the dE/dx resolution is 6% for electrons from Bhabha scattering. The EMC measures photon energies with a resolution of 2.5% (5%) at 1GeV in the barrel (end-cap) region. The time resolution in the TOF barrel region is 68 ps, while that in the end-cap region is 110 ps. The end-cap TOF system was upgraded in 2015 using multigap resistive plate chamber technology. As a result of this upgrading, a time resolution of 60 ps was achieved [18–20]. Approximately 87% of the data used in this analysis benefit from this upgrade.

Simulated samples, generated by the GEANT4-based [22] Monte Carlo (MC) package, which includes the geometric description of the BESIII detector and the detector response, are used to determine the detection efficiency and to estimate the backgrounds. The simulations include the beam energy spread and initial state radiation (ISR) in the e^+e^- annihilation, modeled with the generator KKMC [23]. For ISR simulation, the Born cross section line shape of $e^+e^- \rightarrow \Lambda_c^+ \bar{\Lambda}_c^-$ measured by BESIII is used [24]. Signal MC samples are generated as $\Lambda_c^+ \rightarrow \Sigma^0 K^+ \pi^0$, $\Lambda_c^+ \rightarrow \Sigma^0 \pi^+ \pi^0$, $\Lambda_c^+ \rightarrow \Sigma^0 K^+ \pi^+ \pi^-$, and $\Lambda_c^+ \rightarrow \Sigma^0 \pi^+ \pi^+ \pi^-$, with the $\bar{\Lambda}_c^-$ baryon decays inclusively. The signal decays are produced using the phase space (PHSP) model. To calculate the detection efficiencies, one million signal MC events are generated for each energy point, where Λ_c^+ ($\bar{\Lambda}_c^-$) decays into the signal mode, and $\bar{\Lambda}_c^-$ (Λ_c^+) decays into all possible states. Additionally, to study the peaking background, exclusive MC samples of $\Lambda_c^+ \rightarrow \Xi^0 K^+$ and $\Lambda_c^+ \rightarrow \Lambda K^{*+}$ are generated. Inclusive MC samples consist of open-charm states, ISR production of the J/ψ and $\psi(3686)$ states, and continuum processes $e^+e^- \rightarrow q\bar{q}$ ($q = u, d, s$), used to study backgrounds. The known decay modes of charmed hadrons and charmonium states are modeled with EVTGEN [25, 26] using BFs taken from the Particle Data Group (PDG) [2]; the remaining unknown decays are modeled with LUNDCHARM [27, 28]. Final state radiation from charged final-state particles is incorporated with the PHOTOS package [29].

III. EVENT SELECTION AND DATA ANALYSIS

Owing to the limited availability of data statistics, we adopted a single-tag approach to improve signal efficien-

cies, where only one Λ_c^+ is reconstructed in each event, with no requirement on the recoil side. To avoid potential bias and validate the analysis procedure, a blind analysis was adopted to examine pseudodata; in this analysis, for instance, the inclusive MC sample featured an equivalent size to that of the data. The real data were unblinded after fixing the analysis procedure.

All charged tracks were required to have a polar angle (θ) range within $|\cos\theta| < 0.93$, where θ is defined with respect to the z axis, which is the symmetry axis of the MDC. For those charged tracks not originating from Λ decays, the distance of closest approach to the interaction point (IP) was set to be less than 10 cm along the z -axis, $|V_z|$, and less than 1 cm in the transverse plane, V_{xy} . Particle identification (PID) for charged tracks combines measurements of the energy deposited in the MDC (dE/dx) and the flight time in the TOF to form likelihoods $\mathcal{L}(h)$ ($h = p, K, \pi$) for each hadron h hypothesis. Tracks are identified as protons when the proton hypothesis has the greatest likelihood ($\mathcal{L}(p) > \mathcal{L}(K)$ and $\mathcal{L}(p) > \mathcal{L}(\pi)$), while charged kaons and pions are identified by comparing the likelihoods for the kaon and pion hypotheses, $\mathcal{L}(K) > \mathcal{L}(\pi)$ and $\mathcal{L}(\pi) > \mathcal{L}(K)$, respectively.

The Λ particles were reconstructed from a pair of oppositely charged proton and pion candidates satisfying $|V_z| < 20 \text{ cm}$. The same PID requirements as mentioned before were imposed to select the proton candidates. Other charged tracks were assigned to be π candidates without any PID requirements. These charged tracks were constrained to originate from the common decay vertex by requiring the χ^2 of the vertex fit to be less than 100, and the decay length was required to be greater than twice the vertex resolution away from the IP. To ensure reconstruction reliability, the Λ candidates were required to have an invariant mass within $1.111 < M(p\pi) < 1.121 \text{ GeV}/c^2$, which corresponds to three times the mass resolution around the known Λ mass [2].

Photon candidates were identified using isolated showers in the EMC. The deposited energy of each shower was set to be more than 25 MeV in the barrel region ($|\cos\theta| < 0.80$) and more than 50 MeV in the end cap region ($0.86 < |\cos\theta| < 0.92$). To exclude showers that originate from charged tracks, the angle subtended by the EMC shower and the position of the closest charged track at the EMC were set to be greater than 10° as measured from the IP. To suppress electronic noise and showers unrelated to the event, the difference between the EMC time and event start time was required to be within $[0, 700]$ ns. The π^0 candidates were reconstructed from photon pairs with an invariant mass within $0.115 < M(\gamma\gamma) < 0.150 \text{ GeV}/c^2$. To improve momentum resolution, a one-constraint kinematic fit was utilized to constrain $M(\gamma\gamma)$ to the known π^0 mass [2]. Only combinations that satisfy $\chi^2 < 200$ were retained, and the refined momenta were then employed for subsequent analysis. Then, the Σ^0 can-

candidates were reconstructed from the $\Lambda\gamma$ final states, with an invariant mass in the range $1.179 < M(\Lambda\gamma) < 1.203 \text{ GeV}/c^2$.

To reduce the effect from the noise produced by \bar{p} in the EMC, the opening angle between photon and antiproton was required to be greater than 20° , which was obtained by optimizing the figure-of-merit defined as Punzi FOM = $\frac{\varepsilon}{2.5 + \sqrt{B}}$ [30]. Here, ε is the signal efficiency and B denotes the background yield from the inclusive MC samples. By utilizing the generic event-type analysis tool TopoAna [31], the study of inclusive MC samples shows that the peaking backgrounds for $\Lambda_c^+ \rightarrow \Sigma^0 K^+ \pi^0$ result from $\Lambda_c^+ \rightarrow \Xi^0 K^+$ and $\Lambda_c^+ \rightarrow \Lambda K^{*+}$ decays. These backgrounds involve one less photon in the final state than the signal process. To suppress these backgrounds, we defined the energy difference $\Delta E_{p\pi^-K^+\gamma\gamma} \equiv E_p + E_{\pi^-} + E_{K^+} + E_{\gamma 1} + E_{\gamma 2} - E_{\text{beam}}$, where E_p , E_{π^-} , E_{K^+} , and $E_{\gamma 1/2}$ are the energies of a proton, pion, kaon, and two photons (coming from π^0), respectively, while E_{beam} represents the beam energy. Candidate events for $\Lambda_c^+ \rightarrow \Sigma^0 K^+ \pi^0$ were required to satisfy $-160 < \Delta E_{p\pi^-K^+\gamma\gamma} < -30 \text{ MeV}$, while candidate events for $\Lambda_c^+ \rightarrow \Sigma^0 K^+ \pi^+ \pi^-$ were required to satisfy $\Delta E_{p\pi^-K^+\pi^+\pi^-} < -40 \text{ MeV}$. The distributions of $\Delta E_{p\pi^-K^+\gamma\gamma}$ ($\Delta E_{p\pi^-K^+\pi^+\pi^-}$) are shown in Fig. 2.

After applying the above requirements, the Σ^0 , K^+ , and $\pi^0(\pi^\pm)$ candidates were combined to reconstruct Λ_c^+ . Kinematic variables, including energy difference ΔE , defined as $\Delta E \equiv E_{\text{rec}-\Lambda_c^+} - E_{\text{beam}}$, and the beam-constrained mass M_{BC} , defined as $M_{\text{BC}} \equiv \sqrt{E_{\text{beam}}^2/c^4 - |\vec{p}|^2/c^2}$, were utilized to identify Λ_c^+ candidates. Here, $E_{\text{rec}-\Lambda_c^+}$ and \vec{p} are the energy and momentum of a Λ_c^+ candidate, respectively. If there were multiple combinations satisfying these requirements in an event, the one with the minimum $|\Delta E|$ was retained. Candidate events for $\Lambda_c^+ \rightarrow \Sigma^0 K^+ \pi^0$ and $\Lambda_c^+ \rightarrow \Sigma^0 K^+ \pi^+ \pi^-$ were required to satisfy $\Delta E \in [-27, 6] \text{ MeV}$ and $\Delta E \in [-21, 7] \text{ MeV}$, respectively, with the ranges optimized according to the Punzi FOM.

The signal efficiency and background yield were obtained within the M_{BC} signal region given by $M_{\text{BC}} \in [2.282, 2.291] \text{ GeV}/c^2$. To obtain a pure signal, we employed the truth-match method [32]. This method involves comparing two photons in π^0 , one photon in Σ^0 , and the charged tracks K^\pm and π^\pm with their corresponding truth information. The angle θ_{truth} is defined as the opening angle between each reconstructed track (showers) and its corresponding simulated track (showers). The signal shape was derived from events where θ_{truth} was less than 20° for all tracks (showers).

Table 1 lists the signal efficiencies obtained at different energy points. Figures 3 and 5 show the M_{BC} distributions of the simultaneous fit performed between different energy points for each of the signal decays; no evident Λ_c^+ signals were observed. A likelihood scan method was employed after incorporating the systematic uncertainties, as discussed in the next section, to estimate the upper limits.

The absolute BF of the signal decay is determined by

$$\mathcal{B}^{\text{sig}} \equiv \frac{N_{\Lambda_c^+ \bar{\Lambda}_c^-}^{\text{sig}}}{2 \cdot N_{\Lambda_c^+ \bar{\Lambda}_c^-} \cdot \mathcal{B}^{\text{inter}} \cdot \varepsilon^{\text{sig}}}, \quad (1)$$

where $N_{\Lambda_c^+ \bar{\Lambda}_c^-}$ is the total number of $\Lambda_c^+ \bar{\Lambda}_c^-$ pairs, ε^{sig} is the single-tag efficiency, and $\mathcal{B}^{\text{inter}}$ is the product BFs of the intermediate states Σ^0 , Λ , and π^0 .

Given that there were different distributions of background and signal events at each energy point, a simultaneous fit was performed on individual M_{BC} distributions. The BF of each signal decay was constrained to be the same value through a maximum likelihood simultaneous fit to individual M_{BC} distributions across seven energy points. In the fit, the signal shapes were derived from MC simulations convolved with Gaussian functions to account for the potential difference between data and MC simulations. This is because of the imperfect model-

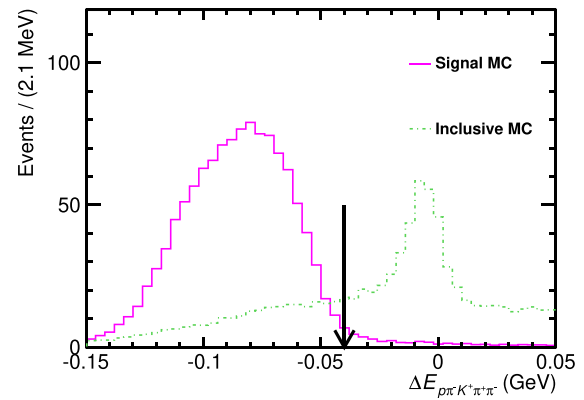
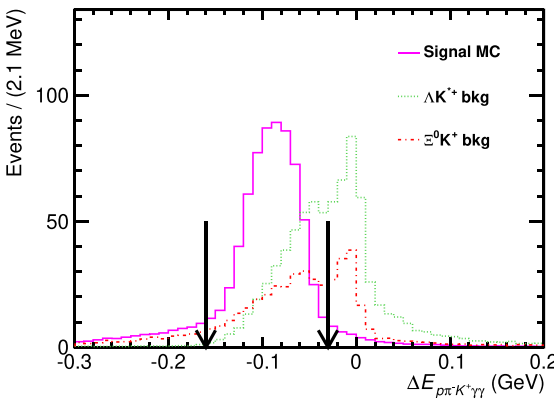


Fig. 2. (color online) Distributions of $\Delta E_{p\pi^-K^+\gamma\gamma}$ ($\Delta E_{p\pi^-K^+\pi^+\pi^-}$) for $\Lambda_c^+ \rightarrow \Sigma^0 K^+ \pi^0$ ($\Lambda_c^+ \rightarrow \Sigma^0 K^+ \pi^+ \pi^-$). The histograms of the signal MC are normalized to make the distribution more intuitive when compared to the inclusive MC.

Table 1. Single-tag efficiencies (%) for $\Lambda_c^+ \rightarrow \Sigma^0 K^+ \pi^0$ and $\Lambda_c^+ \rightarrow \Sigma^0 K^+ \pi^+ \pi^-$ at different energy points; the uncertainties are statistical only.

| \sqrt{s}/MeV | $\varepsilon_{\Lambda_c^+ \rightarrow \Sigma^0 K^+ \pi^0}$ | $\varepsilon_{\Lambda_c^+ \rightarrow \Sigma^0 K^+ \pi^+ \pi^-}$ |
|-----------------------|--|--|
| 4599.53 | 5.17 ± 0.04 | 3.44 ± 0.03 |
| 4611.86 | 4.89 ± 0.03 | 3.10 ± 0.03 |
| 4628.00 | 4.76 ± 0.03 | 3.14 ± 0.03 |
| 4640.91 | 4.76 ± 0.03 | 3.21 ± 0.03 |
| 4661.24 | 4.71 ± 0.03 | 3.32 ± 0.03 |
| 4681.92 | 4.68 ± 0.03 | 3.43 ± 0.03 |
| 4698.82 | 4.65 ± 0.03 | 3.44 ± 0.03 |

ing in MC simulations and the beam-energy spread. The control samples of $\Lambda_c^+ \rightarrow \Sigma^0 \pi^+ \pi^0$ and $\Lambda_c^+ \rightarrow \Sigma^0 \pi^+ \pi^+ \pi^-$ were used to evaluate the resolution. These samples have similar topologies as those of our signal decays. The combinatorial backgrounds are well described by the ARGUS function [33], with the c.m. energy dependent endpoint fixed at E_{beam} . The remaining peaking backgrounds, $\Lambda_c^+ \rightarrow \Xi^0 K^+$ and $\Lambda_c^+ \rightarrow \Lambda K^{*+}$ for $\Lambda_c^+ \rightarrow \Sigma^0 K^+ \pi^0$, were described using exclusive MC simulations with yields determined by the known BFs and the simulated misidentification rates listed in Table 2. For $\Lambda_c^+ \rightarrow \Sigma^0 K^+ \pi^+ \pi^-$, there was no significant peaking background. Unmatched events, studied through the signal MC samples, exhibited a non-flat distribution. In the simultaneous fit, the yields associated with the unmatched events were determined by evaluating the ratio between the matched signal yields and the unmatched background yields, with the ratio obtained from MC simulation.

IV. SYSTEMATIC UNCERTAINTY

The systematic uncertainties in the determinations of the upper limits on the BFs are classified into two categories: additive and multiplicative terms.

The additive terms include the uncertainties introduced by the chosen signal and background shapes. The uncertainty associated with the signal shape was estimated by changing the parameters of the convolved Gaussian functions within their uncertainties. The largest deviation of the individual changes was considered as the uncertainty. The background shape of the non-peaking components was changed from the ARGUS function to be the shape extracted from the inclusive MC samples. The uncertainty due to the fixed contribution of the peaking background yields in the fit was investigated by varying the fixed yields within $\pm 1\sigma$ of the PDG BFs of individual background sources. Among all the above terms, the case yielding the largest upper limit was chosen for further analysis. The additive uncertainty for $\Lambda_c^+ \rightarrow \Sigma^0 K^+ \pi^+ \pi^-$ is dominated by the signal shape uncertainty, while the $\Lambda_c^+ \rightarrow \Sigma^0 K^+ \pi^0$ is mainly influenced by the background shape uncertainty.

The sources of multiplicative systematic uncertainties include tracking and PID of charged particles, π^0 reconstruction, Λ reconstruction, photon reconstruction, ΔE requirement, $\mathcal{B}^{\text{inter}}(\text{Quoted BF})$, MC model, truth matching, MC statistics, $N_{\Lambda_c^+ \bar{\Lambda}_c^-}$, $\Delta E_\Lambda(\Delta E_{p\pi^- K^+ \gamma\gamma}$ and $\Delta E_{p\pi^- K^+ \pi^+ \pi^-}$), and $\theta_{\bar{p}\gamma}$ requirement. The total multiplicative systematic uncertainties are summarized in Table 3 and discussed in detail below.

(a) Tracking and PID: The uncertainties of either PID or tracking of the charged tracks were set to be 1.0% per

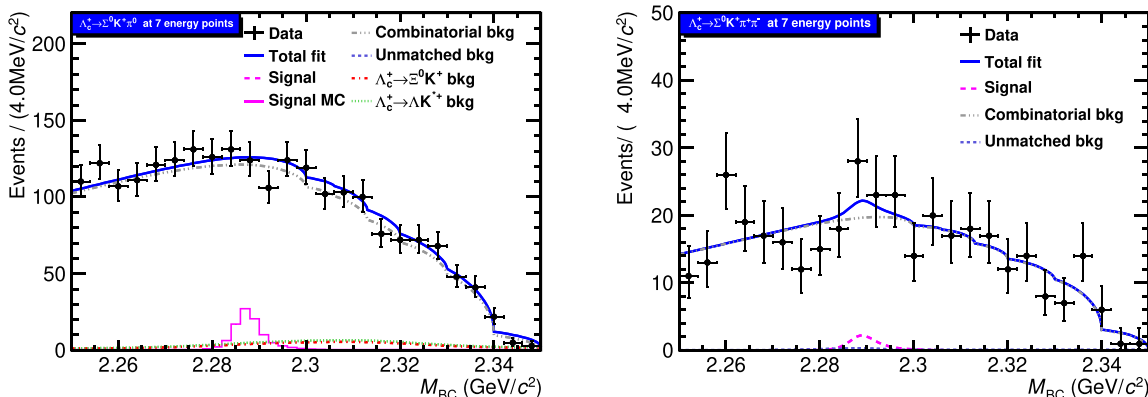


Fig. 3. (color online) Fit to the M_{BC} distributions of $\Lambda_c^+ \rightarrow \Sigma^0 K^+ \pi^0$ (left) and $\Lambda_c^+ \rightarrow \Sigma^0 K^+ \pi^+ \pi^-$ (right) of the combined data. For $\Lambda_c^+ \rightarrow \Sigma^0 K^+ \pi^0$, the violet histograms represent the signal MC samples normalized with a product BF of 1.2×10^{-3} [7]. The ARGUS function includes seven sub-ARGUS functions. The black point with the error bar represents data, the blue solid line represents the total fit function, the gray dashed line represents the combinatorial background, the violet dash line represents the signal function, the navy blue dashed line represents the unmatched component, the cyan dashed line represents the background shape extracted from $\Lambda_c^+ \rightarrow \Lambda K^{*+}$ MC samples, and the red dashed line represents the background shape extracted from $\Lambda_c^+ \rightarrow \Xi^0 K^+$ MC samples.

Table 2. Contamination rates (%) after including the BFs of the secondary decays at each energy point; the uncertainties are statistical only.

| \sqrt{s}/MeV | $\varepsilon_{\Lambda_c^+ \rightarrow \Sigma^0 K^+}$ | $\varepsilon_{\Lambda_c^+ \rightarrow \Lambda K^{*+}}$ |
|-----------------------|--|--|
| 4599.53 | 2.34 ± 0.03 | 2.63 ± 0.02 |
| 4611.86 | 1.97 ± 0.03 | 2.59 ± 0.02 |
| 4628.00 | 2.10 ± 0.03 | 2.58 ± 0.02 |
| 4640.91 | 2.06 ± 0.03 | 2.58 ± 0.02 |
| 4661.24 | 2.10 ± 0.03 | 2.57 ± 0.02 |
| 4681.92 | 2.14 ± 0.03 | 2.56 ± 0.02 |
| 4698.82 | 2.25 ± 0.03 | 2.46 ± 0.02 |

Table 3. Multiplicative systematic uncertainties in unit of % for the BF measurement.

| Source | $\Lambda_c^+ \rightarrow \Sigma^0 K^+ \pi^0$ | $\Lambda_c^+ \rightarrow \Sigma^0 K^+ \pi^+ \pi^-$ |
|-------------------------------------|--|--|
| Tracking | 1.0 | 3.0 |
| PID | 1.0 | 3.0 |
| π^0 reconstruction | 3.1 | - |
| Λ reconstruction | 2.5 | 2.5 |
| Photon detection | 0.5 | 0.5 |
| ΔE requirement | 2.0 | 3.7 |
| MC model | 5.5 | 18.5 |
| $\mathcal{B}_{\text{inter}}$ | 0.8 | 0.8 |
| Truth matching | 5.5 | 4.9 |
| $N_{\Lambda_c^+ \bar{\Lambda}_c^-}$ | 0.9 | 0.9 |
| MC statistics | 0.5 | 0.3 |
| ΔE_Λ requirement | 0.4 | 0.3 |
| $\theta_{\bar{p}y}$ requirement | 0.1 | - |
| Total | 9.2 | 20.1 |

track according to studies of the control sample of $e^+ e^- \rightarrow K^+ K^- \pi^+ \pi^-$ [34].

(b) π^0 reconstruction: The π^0 reconstruction efficiency was studied with the control samples of $\psi(3686) \rightarrow J/\psi \pi^0 \pi^0$ and $e^+ e^- \rightarrow \omega \pi^0$. The associated systematic uncertainty was assigned to be 3.1% for each π^0 .

(c) Λ reconstruction: The systematic uncertainty of Λ reconstruction was assigned to be 2.5% according to the study of $\Lambda_c^+ \rightarrow \Lambda \pi^+$ reported in Ref. [35], which includes the systematics associated with reconstructing the proton and pion daughter particles.

(d) Photon reconstruction: The systematic uncertainty due to the photon reconstruction was estimated to be 0.5% for photons by analyzing the ISR process $e^+ e^- \rightarrow \gamma \mu^+ \mu^-$.

(e) ΔE requirements: Potential differences in the ΔE distributions between data and MC simulation were studied with the control samples of $\Lambda_c^+ \rightarrow \Sigma^0 \pi^+ \pi^0$ and $\Lambda_c^+ \rightarrow \Sigma^0 \pi^+ \pi^+ \pi^-$. The differences between the nominal and alternative acceptance efficiencies, namely 2.0% and 3.7%, were considered as the systematic uncertainties for $\Lambda_c^+ \rightarrow \Sigma^0 K^+ \pi^0$ and $\Lambda_c^+ \rightarrow \Sigma^0 K^+ \pi^+ \pi^-$, respectively.

(f) MC model: The systematic uncertainties associated with the MC model were evaluated with alternative signal MC samples for $\Lambda_c^+ \rightarrow \Sigma^0 K^+ \pi^0$ and $\Lambda_c^+ \rightarrow \Sigma^0 K^+ \pi^+ \pi^-$. These samples were generated as $\Lambda_c^+ \rightarrow \Lambda(1405) K^+$, with $\Lambda(1405) \rightarrow \Sigma^0 \pi^0$ via the PHSP model, and $\Lambda_c^+ \rightarrow \Sigma^0 \pi^+ K^*$, with $K^* \rightarrow K^+ \pi^-$ also simulated in the PHSP model. The differences between the efficiencies of these alternative models and the nominal model were considered as the systematic uncertainties: 5.5% for $\Lambda_c^+ \rightarrow \Sigma^0 K^+ \pi^0$ and 18.5% for $\Lambda_c^+ \rightarrow \Sigma^0 K^+ \pi^+ \pi^-$, respectively.

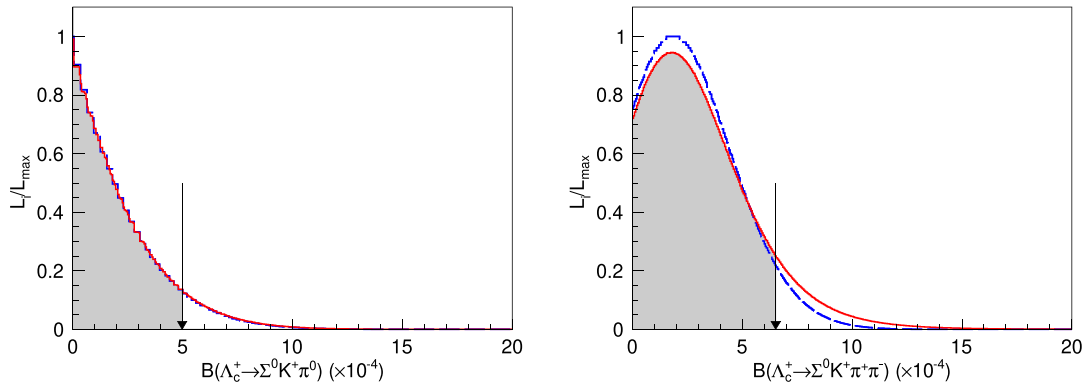


Fig. 4. (color online) Distributions of the likelihoods versus BFs of $\Lambda_c^+ \rightarrow \Sigma^0 K^+ \pi^0$ (top) and $\Lambda_c^+ \rightarrow \Sigma^0 K^+ \pi^+ \pi^-$ (bottom). The results obtained with and without incorporating the systematic uncertainties are represented by red solid and blue dashed curves, respectively. The black arrows show the results corresponding to the 90% C.L.

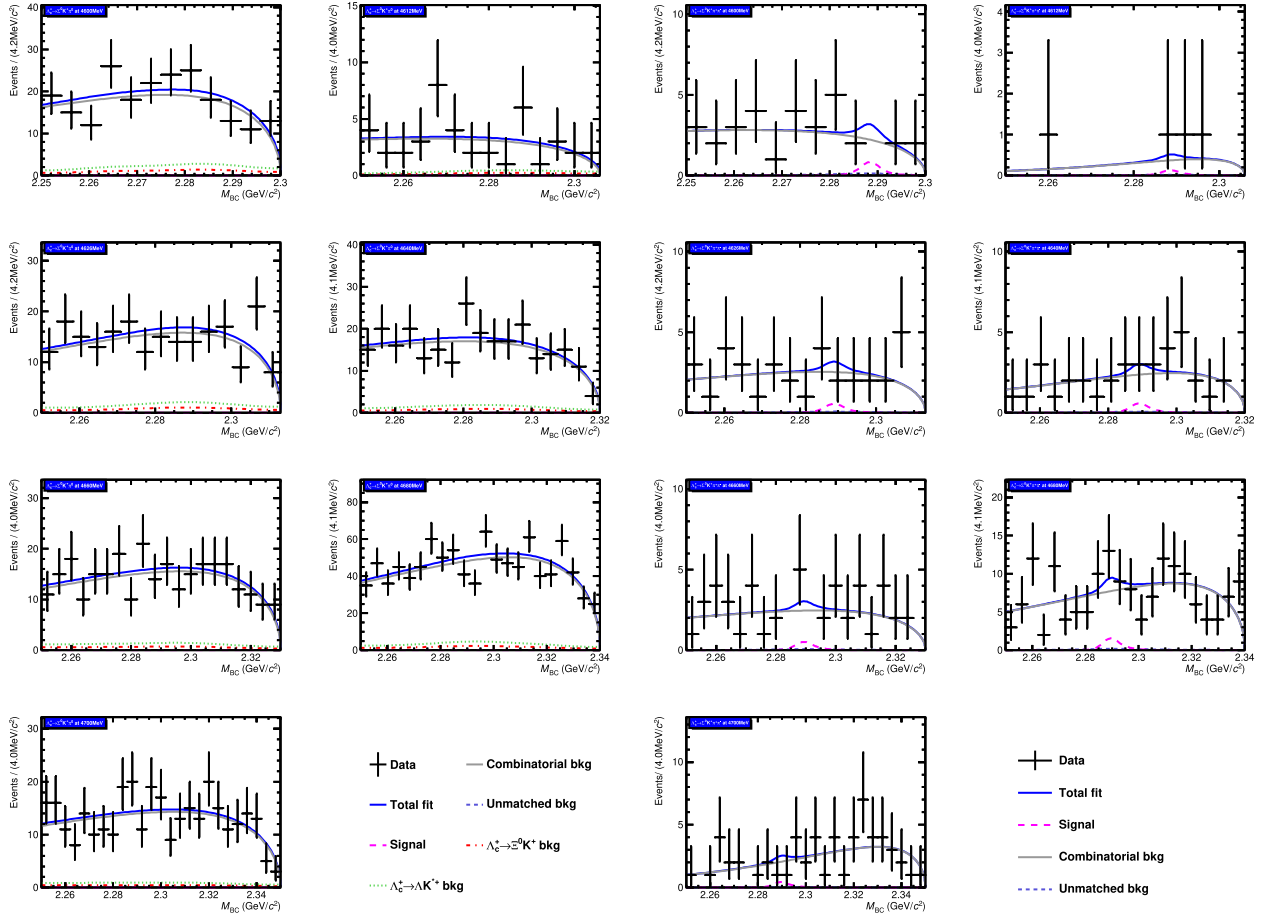


Fig. 5. (color online) Fit to the M_{BC} distributions of $\Lambda_c^+ \rightarrow \Sigma^0 K^+ \pi^0$ (left) and $\Lambda_c^+ \rightarrow \Sigma^0 K^+ \pi^+ \pi^-$ (right) at different energy points. The black point with the error bar represents data, the blue solid line represents the total fit function, the gray dashed line represents the combinatorial background, the violet dash line represents the signal function, the navy blue dashed line represents the unmatched component, the cyan dashed line represents the background shape extracted from $\Lambda_c^+ \rightarrow \Lambda K^{*+}$ MC samples, and red dashed line represents the background shape extracted from $\Lambda_c^+ \rightarrow \Xi^0 K^+$ MC samples.

(g) $\mathcal{B}_{\text{inter}}$: The BFs of $\Sigma^0 \rightarrow \Lambda \gamma$, $\Lambda \rightarrow p \pi^-$ and $\pi^0 \rightarrow \gamma \gamma$ were extracted from results reported by the PDG [2]. The uncertainties of these known BFs add up to a total uncertainty of 0.8%.

(h) Truth matching: To estimate the uncertainty caused by the angle cut in deriving the signal MC shape, we loosened the cut by 5° for each angle. The differences between the nominal and new efficiencies were considered as the systematic uncertainties: 5.5% for $\Lambda_c^+ \rightarrow \Sigma^0 K^+ \pi^0$ and 4.9% for $\Lambda_c^+ \rightarrow \Sigma^0 K^+ \pi^+ \pi^-$.

(i) $N_{\Lambda_c^+ \bar{\Lambda}_c^-}$: The uncertainty of $N_{\Lambda_c^+ \bar{\Lambda}_c^-}$ was extracted from Refs. [13, 15]. Its effect on BF measurement, 0.9%, was assigned as the systematic uncertainty for both decays.

(j) MC statistics: The uncertainties due to limited MC statistics were 0.5% for $\Lambda_c^+ \rightarrow \Sigma^0 K^+ \pi^0$ and 0.3% for $\Lambda_c^+ \rightarrow \Sigma^0 K^+ \pi^+ \pi^-$.

(k) ΔE_Λ requirement: The uncertainty due to the ΔE_Λ requirement was estimated using the control samples of $\Lambda_c^+ \rightarrow \Sigma^0 \pi^+ \pi^0$ and $\Lambda_c^+ \rightarrow \Sigma^0 \pi^+ \pi^+ \pi^-$. The maximum changes of the acceptance efficiencies between data and MC simulation resulting from varying the ΔE_Λ requirement by $\pm 0.05 \text{ GeV}$ were considered as the systematic uncertainties: 0.4% and 0.3% for $\Lambda_c^+ \rightarrow \Sigma^0 K^+ \pi^0$ and $\Lambda_c^+ \rightarrow \Sigma^0 K^+ \pi^+ \pi^-$, respectively.

(l) $\theta_{\bar{p}\gamma}$ requirement: The systematic uncertainty from the $\theta_{\bar{p}\gamma}$ requirement for $\Lambda_c^+ \rightarrow \Sigma^0 K^+ \pi^0$ was estimated using the control sample of $\Lambda_c^+ \rightarrow \Sigma^0 \pi^+ \pi^0$. The maximum change in the acceptance efficiencies between data and MC simulation after varying the $\theta_{\bar{p}\gamma}$ requirement by $\pm 5^\circ$, 0.1% was assigned as the systematic uncertainty.

V. RESULTS

The fit result is consistent with a background-only hypothesis of $\Lambda_c^+ \rightarrow \Sigma^0 K^+ \pi^0$ and $\Lambda_c^+ \rightarrow \Sigma^0 K^+ \pi^+ \pi^-$, and the

upper limits on their BFs were determined. The distributions of raw likelihoods versus individual BFs are represented as blue dashed curves in Fig. 4. Each curve is then convolved with a Gaussian function with zero mean and width set as the corresponding multiplicative systematic uncertainty, according to Refs. [36, 37]. The updated likelihood distributions are represented as red solid lines in Fig. 4. By integrating the red solid curves from zero to 90% of the physical region, the upper limits on the BFs at the 90% C.L. were set to be

$$\mathcal{B}(\Lambda_c^+ \rightarrow \Sigma^0 K^+ \pi^0) < 5.0 \times 10^{-4}, \\ \mathcal{B}(\Lambda_c^+ \rightarrow \Sigma^0 K^+ \pi^+ \pi^-) < 6.5 \times 10^{-4}.$$

VI. SUMMARY

Based on 4.5 fb⁻¹ of e^+e^- annihilation data collected at c.m. energies between 4599.53 MeV and 4698.82 MeV with the BESIII detector at the BEPCII collider, we studied singly Cabibbo-suppressed hadronic decays $\Lambda_c^+ \rightarrow \Sigma^0 K^+ \pi^0$ and $\Lambda_c^+ \rightarrow \Sigma^0 K^+ \pi^+ \pi^-$ using a single-tag method. The upper limits on their BFs at the 90% C.L. were determined to be 5.0×10^{-4} for $\Lambda_c^+ \rightarrow \Sigma^0 K^+ \pi^0$ and 6.5×10^{-4} for $\Lambda_c^+ \rightarrow \Sigma^0 K^+ \pi^+ \pi^-$. The upper limit of the BF of $\Lambda_c^+ \rightarrow \Sigma^0 K^+ \pi^0$ is more stringent than the previous BESIII measurement using a double-tag method [11]. The predictions based on $SU(3)$ flavor symmetry exceed our upper limit by 2.4σ [7], 1.7σ [8], and 2.0σ [9], respectively. These discrepancies can be further investigated through fits to progressively obtain more accurate experi-

Table 4. Comparison of the experimental measurements of $\Lambda_c^+ \rightarrow \Sigma^0 K^+ \pi^0$ and $\Lambda_c^+ \rightarrow \Sigma^0 K^+ \pi^+ \pi^-$ obtained in this study with those of BaBar and BESIII (single-tag) as well as theoretical predictions.

| Decay mode | $\Lambda_c^+ \rightarrow \Sigma^0 K^+ \pi^0$ | $\Lambda_c^+ \rightarrow \Sigma^0 K^+ \pi^+ \pi^-$ |
|-----------------------------|--|--|
| M.Gronau <i>et al.</i> [10] | $(2.1 \pm 0.6) \times 10^{-3}$ | - |
| C.Q.Geng <i>et al.</i> [7] | $(1.2 \pm 0.3) \times 10^{-3}$ | - |
| J.Y.Cen <i>et al.</i> [8] | $(7.8 \pm 2.3) \times 10^{-4}$ | - |
| C.Q.Geng <i>et al.</i> [9] | $(8.2 \pm 1.4) \times 10^{-4}$ | - |
| BESIII (double-tag) [11] | $< 1.8 \times 10^{-3}$ | - |
| BaBar experiment [12] | - | $< 2.5 \times 10^{-4}$ |
| BESIII (single-tag) | $< 5.0 \times 10^{-4}$ | $< 6.5 \times 10^{-4}$ |

mental measurements. Predictions from the statistical isospin model [10] differ from our results by 2.9σ , which indicates that the assumption of $\mathcal{B}(\Lambda_c^+ \rightarrow \Sigma^+ K^+ \pi^-) = \mathcal{B}(\Lambda_c^+ \rightarrow \Sigma^0 K^+ \pi^0)$ is not accurate, as shown in Table 4. For $\Lambda_c^+ \rightarrow \Sigma^0 K^+ \pi^+ \pi^-$, the upper limit is less stringent than the BaBar result [12]. These results provide valuable information for understanding the dynamics of charmed baryon decays and important input to theoretical models. The sensitivities to these two decays could be further improved with a larger data sample at BESIII [21] in the near future.

ACKNOWLEDGEMENTS

The BESIII collaboration thanks the staff of BEPCII and the IHEP computing center for their strong support.

References

- [1] G. S. Abrams *et al.*, *Phys. Rev. Lett.* **44**, 10 (1980)
- [2] S. Navas *et al.* (Particle Data Group), *Phys. Rev. D* **110**, 030001 (2024)
- [3] H. B. Li and X. R. Lyu, *Natl. Sci. Rev.* **8**, nwab181 (2021)
- [4] M. Bauer, B. Stech, and M. Wirbel, *Z. Phys. C* **34**, 103 (1987); Q. P. Xu and A. N. Kamal, *Phys. Rev. D* **46**, 270 (1992)
- [5] H. Y. Cheng, *Z. Phys. C* **29**, 127 (1985)
- [6] G. Meng, S. M. Y. Wong, and F. R. Xu, *J. High Energy Phys.* **11**, 126 (2020)
- [7] C. Q. Geng, Y. K. Hsiao, C. W. Liu *et al.*, *Phys. Rev. D* **99**, 073003 (2019)
- [8] J. Y. Cen, C. Q. Geng, C. W. Liu *et al.*, *Eur. Phys. J. C* **79**, 946 (2019)
- [9] C. Q. Geng, C. W. Liu, and S. L. L, *Phys. Rev. D* **109**, 093002 (2024)
- [10] M. Gronau, J. L. Rosner, and C. G. Wohl, *Phys. Rev. D* **98**, 073003(A) (2018)
- [11] M. Ablikim *et al.* (BESIII Collaboration), *Phys. Rev. D* **109**, 052001 (2024)
- [12] B. Aubert *et al.* (BaBar Collaboration), *Phys. Rev. D* **75**, 052002 (2007)
- [13] M. Ablikim *et al.* (BESIII Collaboration), *Chin. Phys. C* **46**, 113003 (2022)
- [14] M. Ablikim *et al.* (BESIII Collaboration), *Chin. Phys. C* **40**, 063001 (2016)
- [15] M. Ablikim *et al.* (BESIII Collaboration), *Chin. Phys. C* **46**, 113002 (2022)
- [16] M. Ablikim *et al.* (BESIII Collaboration), *Nucl. Instrum. Meth. A* **614**, 345 (2010)
- [17] C. H. Yu *et al.*, *Proceedings of IPAC2016*, (Busan, Korea, 2016)
- [18] X. Li *et al.*, *Radiat. Detect. Technol. Methods* **1**, 13 (2017)
- [19] Y. X. Guo *et al.*, *Radiat. Detect. Technol. Methods* **1**, 15 (2017)
- [20] P. Cao *et al.*, *Nucl. Instrum. Meth. A* **953**, 163053 (2020)
- [21] M. Ablikim *et al.* (BESIII Collaboration), *Chin. Phys. C* **44**, 040001 (2020)
- [22] S. Agostinelli *et al.* (GEANT4 Collaboration), *Nucl. Instrum. Meth. A* **506**, 250 (2003)
- [23] S. Jadach, B. F. L. Ward, and Z. Was, *Phys. Rev. D* **63**, 113009 (2001)
- [24] M. Ablikim *et al.* (BESIII Collaboration), *Phys. Rev. Lett.* **131**, 191901 (2023)

- [25] D. J. Lange, *Nucl. Instrum. Meth. A* **462**, 152 (2001)
- [26] R. G. Ping, *Chin. Phys. C* **32**, 599 (2008)
- [27] J. C. Chen, G. S. Huang, X. R. Qi *et al.*, *Phys. Rev. D* **62**, 034003 (2000)
- [28] R. L. Yang, R. G. Ping, and H. Chen, *Chin. Phys. Lett.* **31**, 061301 (2014)
- [29] E. Richter-Was, *Phys. Lett. B* **303**, 163 (1993)
- [30] Giovanni Punzi, arXiv: [physics/0308063](#)
- [31] X. Y. Zhou, S. X. Du, G. Li *et al.*, *Comput. Phys. Commun.* **258**, 107540 (2021)
- [32] M. Ablikim *et al.* (BESIII Collaboration), *Phys. Rev. D* **109**, 032003 (2024)
- [33] H. Albrecht *et al.* (ARGUS Collaboration), *Phys. Lett. B* **241**, 278 (1990)
- [34] M. Ablikim *et al.* (BESIII Collaboration), *Phys. Rev. D* **99**, 112005 (2019)
- [35] M. Ablikim *et al.* (BESIII Collaboration), *Phys. Rev. Lett.* **116**, 052001 (2016)
- [36] K. Stenson, arXiv: [physics/0605236](#)
- [37] X. X. Liu, X. R. Lyu, and Y. S. Zhu, *Chin. Phys. C* **39**, 103001 (2015)